RJC

RASĀYAN *J. Chem.*
Vol. 18 | No. 2 |997-1003| April - June | 2025
ISSN: 0974-1496 | e-ISSN: 0976-0083 | CODEN: RJCABP
http://www.rasayanjournal.com
http://www.rasayanjournal.co.in

SYNTHESIS AND CHARACTERIZATION OF $AgLaFeO_3$ PEROVSKITE VIA A SIMPLE SOL-GEL METHOD AND INVESTIGATION OF ITS MAGNETIC PROPERTIES

K. Rammohan[1,3,✉], G. VijayaLakshmi[1,2], G. Ramesh[4] and Shuchi Tiwari[5]

[1]Department of Chemistry, University College of Science, Osmania University, Hyderabad-500007, (Telangana), India

[2]Department of Chemistry, Veeranari Chakali Ilamma Women's University, Koti, Hyderabad-500095, (Telangana), India

[3]Department of M.Sc. 5 Year Integrated Chemistry, University P.G. College, Palamuru University, Mahbubnagar-509001, (Telangana), India

[4]Department of Chemistry, Vardhaman College of Engineering, Hyderabad-501218, (Telangana), India

[5]Department of Chemistry, VNR Vignana Jyothi College of Engineering and Technology, Hyderabad-500090, (Telangana), India

✉Corresponding author: patriji2095@gmail.com

ABSTRACT

In this study, silver-doped $LaFeO_3$ ($AgLaFeO_3$) perovskite was genuinely synthesized by a paleoconservative sol-gel method. The results confirmed the blending of silver-doped $LaFeO_3$ perovskite with an orthorhombic structure, crystallizing in the Pnma space group. The Kubelka-Munk analysis demonstrated that Ag^+ doping effectively condensed the band-gap energy of $LaFeO_3$ to 2.37 eV. Furthermore, magnetic studies at room temperature revealed that the $AgLaFeO_3$ perovskite exhibits superparamagnetic behavior, characterized by the absence of magnetization remnant and high saturation levels. Due to these properties, $AgLaFeO_3$ superparamagnetic materials hold significant potential for applications in the medical field.

Keywords: Sol-Gel Method, $AgLaFeO_3$ Perovskite, Powder-XRD, Vibrating Sample Magnetometer Analysis, Superparamagnetic Behavior, Medical Field.

RASĀYAN *J. Chem.*, Vol. 18, No. 2, 2025

INTRODUCTION

The sol-gel process is a commonly used technique to synthesize various perovskite materials effectively. The selection of appropriate A and B cations, as well as chemical doping, plays a critical role in enhancing the stability and selective sensitivity of ABO_3-type perovskite materials. Perovskite, with the general formula ABO_3, is a mineral that can appear in yellow, brown, or black hues. Named after Lev A. Perovski, a Russian mineralogist, who claimed that the mineral was first discovered in the Ural Mountains.[1,2] The cubic crystal structure identified by Perovski corresponds to $CaTiO_3$. Ions form an octahedron around cation B in perovskite crystals, and cation A is in the middle of the BO6 octahedron, joined at the angle of the apex. Anions can coordinate in six dimensions.[3] These materials exhibit remarkable properties, including optoelectronic behavior, half-metallicity, high absorption coefficients, long-range ambipolar charge transport, high dielectric constants, exciton-binding energy, and ferroelectricity[4-6], making them highly versatile for various applications.[7] In this study, $AgLaFeO_3$ perovskite was synthesized using the sol-gel technique and characterized through powder-XRD, FESEM-EDS, VSM analysis, HRTEM analysis, and UV-Vis-DRS. $AgLaFeO_3$'s successful pattern with an orthorhombic crystal structure was validated by the results. Eight O^{2-} atoms in eight-coordinate geometry coordinate with La^{3+} ions in this configuration, and also, $AgLaFeO_3$ perovskite exhibits superparamagnetic behavior.

Doping with noble metals, such as silver, increases oxygen ion vacancies, thereby enhancing the material's catalytic activity. However, limited studies have explored silver doping in submicron particles,

http://doi.org/10.31788/RJC.2025.1829255

flakes, or orthorhombic crystals.[7,8] Such modifications further improve the technological applicability of perovskites. The electrical, magnetic, and structural properties of doped lanthanum oxides are of significant interest due to their relevance in various applications. Among metallic dopants, silver is particularly notable due to its stability in alkaline environments and its ability to enhance the overall electrical conductivity of composites, making it suitable for electrode materials. The sol-gel method offers distinct advantages over other synthesis techniques, such as shorter reaction times and the ability to produce uniformly structured materials with controlled size and shape, making it an efficient and reliable approach for perovskite fabrication.[9]

EXPERIMENTAL

One of the most straightforward methods for creating superior perovskite nano and microstructures is the Sol-Gel process. The method of detailed preparation is given below.

Materials and Methods

Lanthanum(III) nitrate hexahydrate ($La(NO_3)_3 \cdot 6H_2O$) and silver(I) nitrate ($AgNO_3$) were provided by Sisco Pvt. Ltd.'s Research Labs in Taloja, Maharashtra, India. Virat Lab in Mumbai, India, provided us with the nitrate nonahydrate of iron (III) ($Fe(NO_3)_3 \cdot 9H_2O$). Ethanol (C_2H_5OH), ethylene glycol (HO-C_2H_4-OH), citric acid ($HOC(CO_2H)(CH_2CO_2H)_2$), and ammonia (NH_3) were procured from Fine-Chem Industries, Mumbai, India. All chemicals were of AR grade for high grade of quality chemicals.

Scheme for the Preparation of AgLaFeO3 Perovskite Materials

Synthesis of AgLaFeO3 Perovskites by the Sol-Gel Method

The perovskite $AgLaFeO_3$ powder was produced by the sol-gel technique, which was then Calcination. Initially, 0.09 g of $AgNO_3$, 5 g of $La(NO_3)_3 \cdot 6H_2O$ (0.05:0.95 ratio), and 4.6 g of $Fe(NO_3)_3 \cdot 9H_2O$ were soluble in 200 mL of Et-OH and stirred continuously at 27o °C for two hours. After this, 0.5 g of citric acid was added to the mixture, and stirring was continued. To adjust the pH to 7, an NH3 solution was introduced, followed by one hour of stirring at 70°C. Afterward, 1 mL of ethylene glycol was added to the reduced 50% solution (100 mL) and stirred for an additional hour at 160°C. The resulting mixture was dried, ground into fine particles, and subjected to calcination in a muffle furnace at 800°C for eight hours. The final product was obtained as 98% $AgLaFeO_3$ perovskite material.

Reaction Involved in the Synthesis of $AgLaFeO_3$ Perovskite Material

$$La(NO_3)_3.6H_2O + AgNO_3 + Fe(NO_3)_3.9H_2O + C_6H_8O_7.H_2O \longrightarrow AgLaFeO_3 + 6CO_2 + 3N_2 + nH_2O \quad 98\%\ yield$$

RESULTSANDDISCUSSION

UV-Visible Diffuse Reflectance Spectroscopy Analysis

Figure-1 presents the UV-visible DRS spectrum of $AgLaFeO_3$ synthesized via the sol-gel method, with absorbance plotted against wavelength. The absorption edge of $AgLaFeO_3$ was observed at 774 nm. The spectrum exhibits a red shift, indicating an absorption shift toward a longer wavelength. This shift confirms a reduction in the band gap energy, as wavelength is inversely proportional to band gap energy.[10] The narrowing of the band gap promotes electron excitation between the conduction and valence band with lower energy input, thereby enhancing the photocatalytic activity of $AgLaFeO_3$.

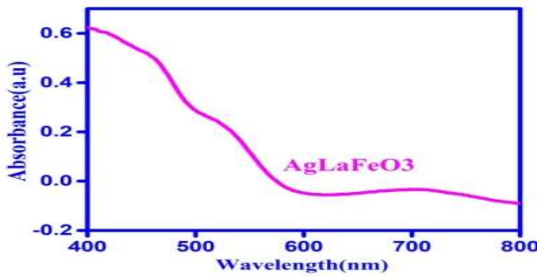

Fig.-1: UV-visible DR Sspectrum of $AgLaFeO_3$ Material

Band Gap Energy Analysis

The Kubelka-Munk (KM) plot is used to estimate the band gap energy from intensity vs. energy plots. The band-gap energy (Eg) was calculated using the formula: Example -1240/2, where Eg is the band gap energy and λ is the wavelength of the absorption edge[11]. The band gap was measured. The band-gap energy of AgLaFeO, perovskite materials synthesized via the sol-gel method, was determined from their respective KM plots (Fig.-2). The KM plot for AgLaFeO exhibited a band gap of 2.37 eV, which is significantly lower than the band-gap energy of LaFeO (2.94 eV). This reduction in band gap energy demonstrates the effective incorporation of Ag ions into the LaFeO lattice. A lower band gap enhances electron excitation from the valence band to the conduction band, resulting in hole formation in the valence band. This enhanced charge carrier mobility suggests that silver ions were successfully doped into LaFeOs, further improving its optoelectronic and photocatalytic properties.

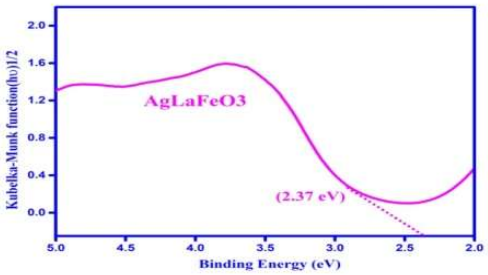

Fig.-2: KM Plot of$AgLaFeO_3$ Perovskitematerial

X-ray Diffraction Analysis

Figure-3 shows the X-ray diffraction (XRD) spectra of silver-doped $LaFeO_3$ perovskite materials calcined at 800 °C. Silver-doped $LaFeO_3$ exhibits an intense peak at a 2θ value of 32.4 degrees corresponding to the (12 1) h, k, and l planes, indicating an orthorhombic phase. Therefore, this demonstrates that silver ions are successfully doped into the $LaFeO_3$ crystal.[12]

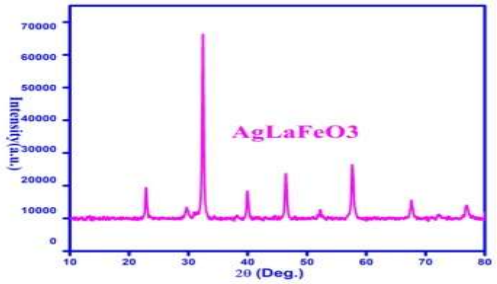

Fig.-3: The XRD Patterns of Ag LaFeO3 Perovskite Material

FESEM and EDS Analysis

The FESEM and EDS were used to examine pure AgLaFeO3 perovskite to examine its surface morphology and elemental analysis. After silver (Ag) doping, the shape of $AgLaFeO_3$ changed dramatically, as large, irregularly shaped lumps are shown in Fig.-4. It indicates that silver ions are doped in $LaFeO_3$ and form AgLaFeO3.13 EDS analysis revealed that the chemical ratios of La, Ag, Fe, and O in pure powders of AgLaFeO3 synthesized by the sol-gel method are stoichiometric, with percentage weights of each element shown in Table-1. The EDS analysis shows a silver (Ag) concentration of 7.42 wt%.

HRTEM Analysis

To understand the three-dimensional structural morphology of $AgLaFeO_3$ perovskite synthesized by the sol-gel technique, Fig.-5 presents HRTEM images. These images reveal that the silver nanoparticles are well-assembled on the surface of the $LaFeO_3$ perovskite, with flawless crystal lattice fringes[13]. The interplanar distance between these fringes is 0.28 nm, corresponding to the (121)[14] crystal plane of silver (Ag). The crystalline silver nanoparticles show no noticeable internal defects, suggesting high crystallinity.

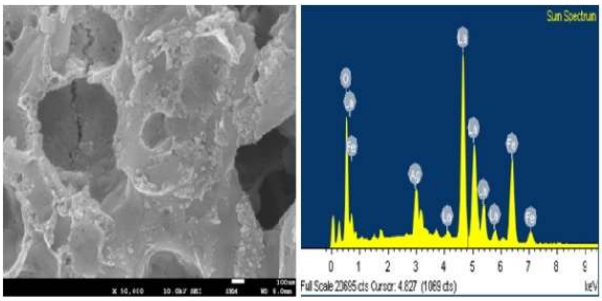

Fig.-4: FESEM and EDS Images of $AgLaFeO_3$ Materials

Additionally, Fig.-5 includes SAED patterns of silver-doped $LaFeO_3$.

Table-1: EDS of $AgLaFeO_3$ Perovskite Material

Element	Weight%	Atomic%
O K	18.76	59.82
Fe K	17.49	15.98
Ag L	7.42	3.51
La L	56.33	20.69
Total	100.00	

The SAED patterns of pure $LaFeO_3$ exhibit weak diffraction rings or spots, which can be attributed to the existence of silver. In contrast, the SAED patterns of $AgLaFeO_3$ show polycrystalline diffraction rings, further confirming the successful doping and uniform distribution of silver in the perovskite lattice.

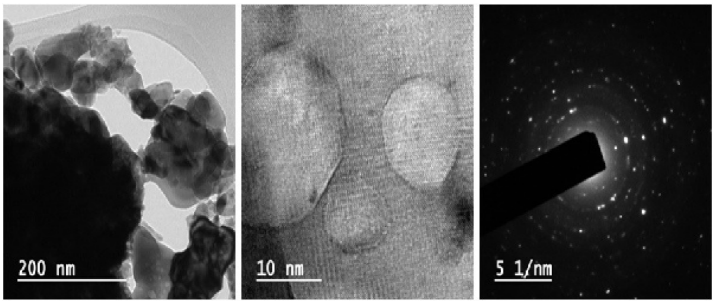

Fig.-5: HRTEM Images and Selected Area Electron Diffraction (SAED) Patterns of $AgLaFeO_3$ Materials

XPS Analysis

To obtain a better comprehension of the surface architecture and chemical valence states of key elements in $AgLaFeO_3$, an XPS analysis was conducted, as shown in Fig.-6. Figure-6a presents the XPS survey spectra of $AgLaFeO_3$ perovskite, confirming the presence of lanthanum (La), silver (Ag), iron (Fe), and oxygen (O) in the sample, with no additional elemental peaks observed, indicating the purity of the material. Silver (Ag) exhibits two prominent signals at 367.71 eV and 373.81 eV, indicating that Ag is in the +1 oxidation state. Shifts in the binding energy are observed due to Ag doping[15], as shown in Fig.-6b. Lanthanum (La) displays two significant signals at 835.86 eV and 865.27 eV, which are assigned to the La $3d_{5/2}$ and La $3d_{3/2}$ binding energies, respectively. These values are close to the standard values for La $3d_{5/2}$ (836.0 eV) and La $3d_{3/2}$ (853.0 eV), as shown in Fig.-6c.[16] This corresponds to the La^{2+} oxidation state in the oxide structure. Iron (Fe) is present in the Fe^{3+} oxidation state, as shown in Figure 6d. The binding energies for the Fe $2p_{3/2}$ and Fe $2p_{1/2}$ peaks are observed at 710.86 eV, 724.70 eV, and 743.01 eV, which correspond to the Fe^{3+} oxidation state (standard values: Fe $2p_{3/2}$ - 869.3 eV; Fe $2p_{1/2}$ - 852.6 eV). Additionally, the La 3d and Fe 2p peaks shift slightly towards lower and higher binding energies, respectively, compared to typical peak values[17,18], indicating La-Fe interactions. Oxygen (O) shows two peaks at 528.55 eV and 531.17 eV, which confirm the presence of O^{2-} in the $AgLaFeO_3$ perovskite lattice, as depicted in Fig.-6e. These peaks align with the expected chemical structure of $AgLaFeO_3$. Overall, the XPS analysis reveals the successful doping of silver into the $LaFeO_3$ perovskite and confirms the oxidation states of the constituent elements.

VSM Analysis

The magnetic behavior of $AgLaFeO_3$ perovskite, synthesized via the sol-gel technique, was analyzed and is shown in Fig.-7, which depicts the hysteresis loops of magnetization (M) versus field (H) obtained using a VSM analysis at 25°C.[19] The result reveals a substantial ferromagnetic effect, with enhanced magnetization compared to bulk materials. This behavior is attributed to the probability distribution of Fe^{3+} ions within the octahedral structure, as suggested by Gehring and Goodenough. At room temperature, the magnetic study indicates that the $AgLaFeO_3$ perovskite exhibits superparamagnetic behavior. These superparamagnetic materials do not exhibit permanent magnetization and demonstrate high saturation magnetization, making them suitable for a range of medical applications.[20,21,22]

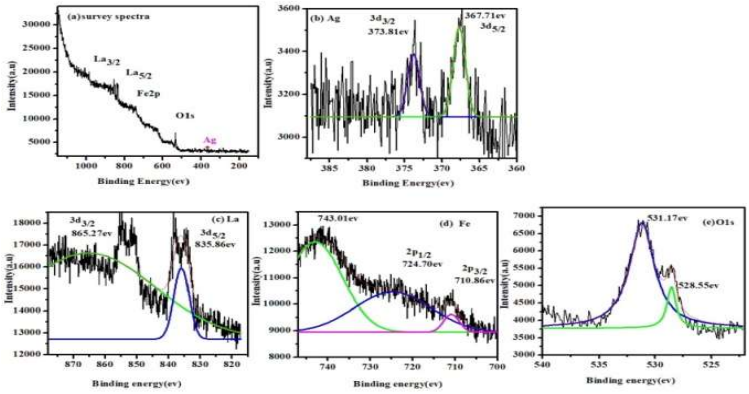

Fig.-6: The XPS Spectrum of $AgLaFeO_3$ Material (a) Survey Spectra, (b) Ag 3d, (c) La 3d, (d) Fe 2p and (e) O 1s

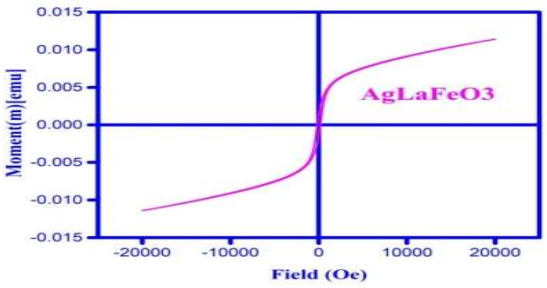

Fig.-7: VSM of Silver Doped $LaFeO_3$ Perovskite Materials

CONCLUSION

$AgLaFeO_3$ perovskite was synthesized by a simple and traditional sol-gel process followed by calcination. FESEM analysis reveals that the $AgLaFeO_3$ exhibits a large, irregular morphology, which significantly differs from that of pure $LaFeO_3$, suggesting that the silver ions have effectively modified the material's structure. XRD results confirm the synthesis of silver ions into the $LaFeO_3$ crystal lattice. EDS analysis shows that the silver content is 7.42 wt%, while HRTEM imaging displays a well-dispersed arrangement of silver nanoparticles on the surface of $LaFeO_3$ particles. XPS analysis indicates no significant change in the oxidation state of iron, but a slight shift in the oxidation state of lanthanum, suggesting that silver ions are doped onto the La site. The Kubelka-Munk plot further demonstrates that silver doping effectively reduces the band gap energy of $LaFeO_3$, lowering it to 2.37 eV. VSM analysis results show that the $AgLaFeO_3$ exhibits superparamagnetic behavior at room temperature, characterized by no magnetization remnant and high saturation levels. These superparamagnetic properties highlight the potential of $AgLaFeO_3$ in various applications, particularly in the medical field and other areas that require magnetic materials.

ACKNOWLEDGMENTS

The authors would like to express their gratitude to the Department of Chemistry, Osmania University, CFRD-OU, for providing the necessary infrastructure, and also gratitude to the Department of M.Sc. 5-year integrated chemistry, Palamuru University, for financial support.

CONFLICT OF INTERESTS

The authors declare that they have no known competing financial interests or personal relationships that could have appeared to influence the work reported in this paper.

AUTHOR CONTRIBUTIONS

All the authors contributed significantly to this manuscript, participated in reviewing/editing and approved the final draft for publication. The research profile of the authors can be verified from their ORCID ids, given below:

K. Rammohan https://orcid.org/0000-0001-8994-905X
G. Vijaya Lakshmi https://orcid.org/0000-0001-7183-4908
G. Ramesh https://orcid.org/0000-0002-5630-4383
ShuchiTiwari https://orcid.org/0000-0002-5585-4818

REFERENCES

1. D. Shi, V. Adinolfi, R. Comin, M. Yuan, E. Alarousu, A. Buin, Y. Chen, S. Hoogland, A. Rothenberger, K. Katsiev, Y. Losovyj, X. Zhang, P. A. Dowben, O. F. Mohammed, E. H. Sargent, and O. M. Bakr, *Science*, **347**, 519(2015), https://doi.org/10.1126/science.aaa2725
2. G. Ravi, V. Naveen Kumar, V. Radha, G. Ravinder, P. Someshwar, and M. Vithal, *International Journal of Applied Ceramic Technology*, **12(3)**, 700(2015), https://doi.org/10.1111/ijac.12250
3. Z. Mesikova, P. Sulcova & M. *Journal of Thermal Analysis and Calorimetry,* **91**, 163(2008). https://doi.org/10.1007/s10973-007-8312-4
4. W.S. Yang, B.W. Park, E.H. Jung, N.J. Jeon, Y.C. Kim, D.U. Lee, S.S. Shin, J. Seo, E.K. Kim, J.H. Noh, S.I. Seok, *Science*, **356**, 1376(2017), https://doi.org/10.1126/science.aan2301
5. N. Ahn, D.Y. Son, I.H. Jang, S.M. Kang, M. Choi, N.G. Park, *Journal of the American Chemical Society*, **137**, 8696(2015), https://doi.org/10.1021/jacs.5b04930
6. S. Zhao, B. Zhao, Y. Chen, G. Yang, and X. Li, *ACS Applied Energy Materials*, **2**, 6230(2019), http://doi.org/10.1021/acsaem.9b00757
7. Z.N. Garba, W. Zhou, M. Zhang, and Z. Yuan, *Chemosphere*, **244**, 125474(2020), https://doi.org/10.1016/j.chemosphere.2019.125474
8. Q. Jiang, Y. Zhao, X. Zhang, X. Yang, Y. Chen, Z. Chu, Q. Ye, X. Li, Z. Yin, and J. You, *Nature Photonics*, **13**, 460(2019), https://doi.org/10.1038/s41566-019-0398-2
9. J. Cheng, and A. Navrotsk, *Chemistry of Materials,* **17(8),** 2197(2005), https://doi.org/10.1021/cm048613o
10. V. R. Choudhary, B. S. Uphade, and S. G. Pataskar, *Fuel*, **78(8),** 919(1999), https://doi.org/10.1016/S0016-2361(99)00007-1
11. F. Riosco, L. Radov, X. Gordon, A. Garcia and G. Pecchi, *The Journal of the Chilean Chemical Society*, **55(1)**,44(2010), http://dx.doi.org/10.4067/S0717-97072010000100011
12. G.A.H. Mekhemer, H.A.A. Mohamed, and A. Bumajdad, *Scientific Reports,***1**, 7453(2023), https://doi.org/10.1038/s41598-023-34065-3
13. S.B. Hammouda, F. Zhao, , Z. Safaei, D. L. Ramasamy, B. Doshi, & M. Sillanpaa, *Applied Catalysis B: Environmental*, **233**, 99(2018), https://doi.org/10.1016/j.apcatb.2018.03.088
14. X.T. Yin, H. Huang, J.L. Xie, D. Dastan, J. Li, Y. Liu, X.M. Tan, X.C. Gao, W.A. Shah, and X.G. Ma, *Green Chemistry Letters and Reviews,* **15(3)**, 546(2022), https://doi.org/10.1080/17518253.2022.2112093
15. E.K. Abdel-Khalek, M.A. Motawea, A.M. Aboelnasr and H.H. El-Bahnasawy, *Physica B: Condensed Matter,* **624**, 413415(2022), https://doi.org/10.1016/j.physb.2021.413415
16. Q. Liu, Z. You, S. Zeng, and H. Guo, *Journal of Sol-Gel Science and Technology*, **80**, 860(2016) https://doi.org/10.1007/s10971-016-4141-x

17. B.J. Kim, E. Fabbri, D.F. Abbott, X. Cheng, A.H. Clark, M. Nachtegaal, M. Borlaf, I.E. Castelli, T. Graule, and T.J. Schmidt, *Journal of the American Chemical Society*, **141(13)**, 5231(2019), http://dx.doi.org/10.1021/jacs.8b12101
18. Y.Ye.H. Yang, R. Li, X. Wangh, *Journal of Sol-Gel Science and Technology*, https://doi.org/10.1007/s10971-017-4332
19. G. Zhang, G. Liu, L. Wang, J.T.S. Irvine, *Chemical Society Reviews*, **45**, 5951(2016), https://doi.org/10.1039/C5CS00769K
20. B.J. Kim, E. Fabbri, D.F. Abbott, X. Cheng, A.H. Clark, M. Nachtegaal, M. Borlaf, I.E. Castelli, T. Graule, and T.J. Schmidt, *Journal of the American Chemical Society*,**141(13)**, 5231(2019), https://doi.org/10.1021/jacs.8b12101
21. F.Yang, X.Yang, K. Su, J. Lin, Y. H. and Q. Lin, *Molecules* , **28**, 5745(2023), https://doi.org/10.3390/molecules28155745
22. L. Karoui, M. Smari, and T. Mnasri, *The Royal Society of Chemistry,***14(16)**, 11456(2024), https://doi.org/10.1039/D4RA01086H

[RJC-9255/2025]